

Near-Infrared Spectroscopy as a Tool for Simultaneous Determination of Diesel Fuel Improvers

Ivana Hradecká,* Aleš Vráblík, Jakub Frątczak, Nikita Sharkov, Radek Černý, and Vladimír Höinig



Cite This: *ACS Omega* 2023, 8, 4038–4045



Read Online

ACCESS |



Metrics & More

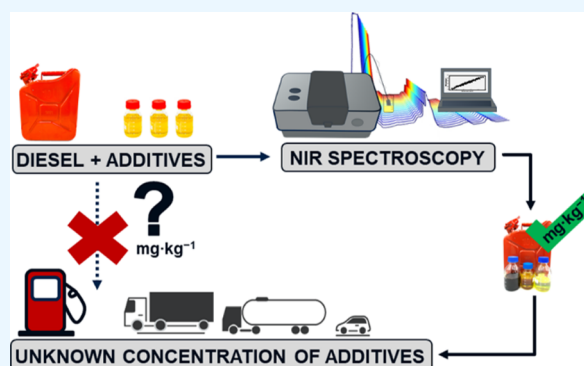


Article Recommendations



Supporting Information

ABSTRACT: Diesel and biodiesel blends requires additives to improve fuel quality properties and engine performance. Diesel improvers are added before, during and/or after the fuel is blended. However, no accurate rapid and non-destructive analytical method is used during the fuel production that could determine the exact concentration of various types of improvers in diesel fuel. Thus, the aim of this study was to determine the concentration of several improvers in diesel matrices at the same time. Three types of diesel improvers, i.e., a cold-flow improver (CFI), a conductivity–lubricity improver (CLI), and a cetane number improver (CNI), were simultaneously determined by near-infrared (NIR) spectroscopy combined with multivariate statistical analysis and the partial least squares algorithm. The prediction models yielded high correlation coefficients (R^2) >0.99 and satisfactory values of the root mean square error of calibration as follows: CLI 4.2 ($\text{mg}\cdot\text{kg}^{-1}$), CFI 4.6 ($\text{mg}\cdot\text{kg}^{-1}$), and CNI 5.3 ($\text{mg}\cdot\text{kg}^{-1}$). The residual standard deviation of the repeatability was calculated to be around 8%. These results highlight the potential of NIR spectroscopy for use as a fast, low-cost, and efficient tool to determine the concentrations of diesel improvers. Moreover, this technique is suitable for application during refinery production, especially for the purpose of online monitoring to prevent overdoses of additives and save financial expenses.



1. INTRODUCTION

In the last decade, the emission of environmental pollutants upon the combustion of fossil fuels has become of significant concern. These concerns have resulted in stricter global fuel regulations, particularly in terms of reducing the emission of sulfur, nitrogen oxides (NO_x), carbon monoxide, total hydrocarbons, and particulate matter from the combustion of diesel fuels.¹ In addition, the shift to renewable sources to replace fossil fuels has also accelerated, leading to the increased production, improvement, and use of environmentally friendly biofuels.

However, the use of biofuels has been shown to have a negative effect on the properties and behavior of the fuel inside the engine due to the absence of specific components. As a result, cost-effective additization is necessary to maintain the desirable properties of diesel fuels while ensuring an optimal engine performance. Fuel additives, i.e., improvers, come in several types, such as liquids, gases, or solid additives. In general, additives are divided into different categories (cetane improvers, antioxidants, metal-based additives, lubricity improvers, etc.) and differ in effects and applications.²

More specifically, additives can be mixed into the fuel either during blending or after blending to improve the fuel properties without requiring major changes to current engine technologies. Furthermore, these chemicals are effective even when added at low concentrations. However, no purposeful

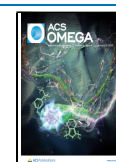
regulations exist regarding the concentrations of such fuel improvers that can be added to diesel, which can lead to an unnecessarily high consumption of improvers and higher costs.³ This issue could potentially be solved by the use of near-infrared (NIR) spectroscopy to effectively and simultaneously determine the concentrations of diesel improvers within the diesel matrix, while also purposefully correcting their concentrations during online monitoring.

NIR spectroscopy is a well-known analytical technique that has proven its potential for use in the refinery industry, wherein it has been developed for various fuel characterization applications over the last decade. This technique is desirable because of its rapid, nondestructive, and low-cost nature, in addition to its potential for combination with multivariate statistical analysis. Furthermore, the NIR technique can be integrated into portable devices that can be used directly for online monitoring or off-site operations.^{4,5} Indeed, a combination of NIR spectroscopy and multivariate analysis is

Received: October 24, 2022

Accepted: January 5, 2023

Published: January 19, 2023



often used to determine the chemical and physical properties of fuels and their components.^{6–11}

Three main types of diesel improvers are commonly employed, including cold-flow improvers (CFIs), conductivity–lubricity improvers (CLIs), and cetane number improvers (CNIs); however, no method exists that permits the simultaneous determination of all three additive types. In terms of their application, the CFI additive improves the flow of diesel fuel in cold weather and enhances the cold-flow properties of diesel fuels, including the cloud point, pour point, and cold filter plugging point.¹² The main problem with diesel fuel is its tendency to exhibit reduced flow at reduced temperatures, and this can be attributed to the formation of solids in the cold fuel.¹³ For example, wax crystals can be generated, which possess a slightly higher density than diesel fuel at any given temperature, and so there is a tendency for wax to settle at the bottom of the storage vessel. The resulting reduction in the fuel flow therefore affects the transport and combustion of such distillate fuels in internal combustion engines. To avoid such issues, CFIs are commonly employed, including wax antissettling flow improvers (WAFI) that reduce wax crystal formation while also exhibiting an antissettling effect.¹⁴

In addition, the CLI is a combination of diesel additives that focus on improving the lubrication and electric conductivity of the fuel while allowing the electrostatic buildup to dissipate safely without sparking.^{15,16} This combination additive is commonly employed due to the fact that low-lubricity diesel can cause premature failure of injection system components and reduce engine performance. To determine the lubricity of a fuel, a number of analytical methods have been reported, including the high-frequency reciprocating rig method according to European standard (EN) 590:2013+A1:2017 and American Society for Testing Materials (ASTM) D6079-18.^{17,18} Moreover, when the sulfur content of diesel fuel is reduced to meet the necessary requirements, a variety of engine problems can arise, including increased wear, injector corrosion, engine instability, or slow starting.¹⁹ These problems arise because of the removal of naturally occurring conductive polar substances during the hydrodesulfurization process, ultimately resulting in a low diesel conductivity.²⁰

The cetane number of diesel, which is an indicator of the speed of combustion of diesel fuel and the compression required for ignition, can be improved by the addition of a booster CNI, such as alkyl nitrates. The most common type used is 2-ethylhexyl nitrate (EHN).²¹ This additive is used due to its rapid decomposition in the combustion chamber at high temperatures, in addition to the fact that it generates products that help initiate combustion and shorten the ignition delay time. What is more, it contributes to lower NO_x.²² According to previous reports, the addition of 0.1 wt % EHN can increase the cetane number of diesel by between 4 and 6.^{23–25} Importantly, EHN is effective at low concentrations, which is important when the maximum percentage of added improvers cannot exceed 5%.²⁶

Therefore, the aim of this study is to verify whether it is possible to determine the concentrations of three types of diesel improvers at the same time in diesel fuel by NIR spectroscopy combined with multivariate statistical analysis and the partial least squares (PLS) algorithm.

2. EXPERIMENTAL SECTION

2.1. Sample Collection and Preparation. A mixture of hydrogenated middle distillates (gas oil and kerosene) was used as the fuel matrix, which is referred to hereafter as diesel. The diesel specimen was produced by processing a mixture of Russian export blend and Caspian Pipeline Consortium crude oil in an 80:20 wt % ratio using commercial refinery technology.

The diesel sample was extracted on a static mixer (blender) according to the standard procedure to ensure that it did not contain any additives or fatty acid methyl esters and to ensure that it would only contain laboratory-added amounts of selected additives.²⁷ With the exception of the cold-flow properties, the lubricity, and the cetane number, which are normally modified by additives, the diesel sample met all quality requirements outlined in EN 590:2013+A1:2017.

Three commercially available additives were used in this study. More specifically, CFI, the additive for modifying cold-flow properties (CFPP parameter) of the WAFI type, consisted of a mixture of vinyl acetate, ethylene copolymers, and modified polymers, while the CLI was composed of fatty acids, including linoleic and oleic acids, and 2-ethylhexyl nitrate (2-EHN, >99%) was used as the CNI.

All diesel samples were prepared on a laboratory scale. In each case, the desired additive was homogenized and the appropriate mass was placed in a small glass beaker. The beaker was then placed in a dryer for 15–20 min at the temperature recommended by the additive manufacturer (i.e., 40 °C for the CFI, 50 °C for the CLI, and ambient temperature 21–23 °C for the CNI). The additive was then quantitatively transferred from the beaker to a preheated (45 °C) diesel sample of the required calculated weight. The total amount was 10 g for one analyzed sample. The final samples were thoroughly homogenized and analyzed, as detailed below.

2.2. NIR Data Acquisition and Modeling. Each sample (~10 mL) was analyzed under laboratory conditions using a Nicolet 6700 Fourier transform infrared (FTIR)/NIR spectrometer (Thermo Fisher Scientific, Waltham, Massachusetts, USA) equipped with an immersion probe (Hellma GmbH & Co. KG, Müllheim, Germany) with a 5 mm optical path and an InGaAs detector. The spectra were acquired in the spectral range of 10,000–4000 cm⁻¹ and are displayed as the average of three consecutive measurements from 50 scans with a resolution of 8 cm⁻¹. These spectra were then subsequently employed for NIR model development. OMNIC software (Thermo Fisher Scientific, Waltham, Massachusetts, USA) was used for all spectral analyses. The chemometric computations were performed using TQ Analyst 9 software (Thermo Fisher Scientific, Waltham, Massachusetts, USA) for the quantitative determination of the diesel improvers.

NIR models were developed based on the PLS algorithm, as it allows the compression of large spectral data.

On top of this, the number of spectral variables is converted to a smaller number of factors in the spectral matrix, thereby removing unnecessary spectral information. PLS uses the relationship between the observed response variable y (y -variable = additive concentration) and the independent variable x (x -variable = NIR spectral matrix), displaying linear distributions for the calibration standards, with correlation coefficients close to 1. The PLS calibration model for the mean-centered data was assessed using the root mean square error of calibration (RMSEC), which indicates the quality of a

calibration model, and the root mean square error of cross-validation (RMSECV) using the leave-one-out method, where one standard was always removed and subsequently predicted by the model prior to comparison with the actual value, as follows:

$$\text{RMSE} = \sqrt{\frac{\sum_i^n (y_i - \hat{y}_i)^2}{n}}$$

where y_i is the actual value, \hat{y}_i is the predicted value, n is the total number of samples in the calibration set for the RMSEC, and n also represents the number of samples in the cross-validation set for the RMSECV.²⁸ In addition, the dependence of the latent variables (LVs) on the PLS-based RMSECV was determined using the minimum value of the predicted residual error sum of squares (PRESS).

To determine the quality of the model and verify whether the NIR measurements are fit for purpose, the ratio of error range (RER) of the calibration set was calculated as the ratio of the maximum and minimum of the reference data to the RMSECV, and the ratio of prediction to deviation (RPD), which in turn was defined as the ratio between the standard deviation (SD) of the reference data from the external cross-validation set by the RMSECV.^{29,30}

Moreover, a number of statistical parameters were evaluated, including an external validation dataset of 10 samples, which were not included in the calibration set, and a repeatability test along with its residual standard deviation (RSD), which was performed over a short time period under identical NIR conditions. Calibration standard number 119 was measured 15 times, and the NIR immersion probe was cleaned and then reinserted into the sample. The workflow scheme of building the PLS model is presented in Figure 1.

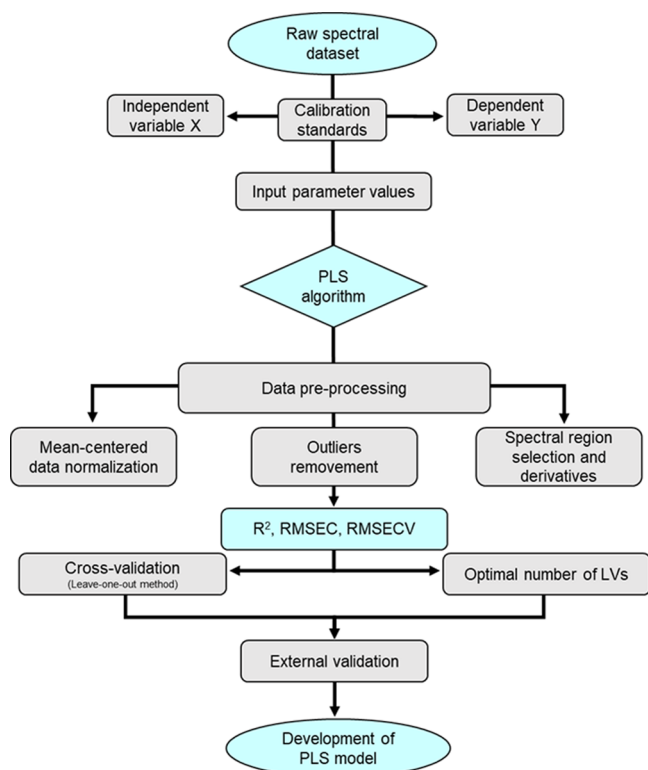


Figure 1. Workflow scheme of building a PLS model.

3. RESULTS AND DISCUSSION

3.1. Preprocessing of the NIR Spectra. The raw spectra of all samples shown in Figure 2a were obtained in the region of 10,000–4000 cm^{-1} . The absorbance spectra acquired across the NIR spectral range were inspected to identify gross outliers and noisy spectral regions. Generally, regions in the given NIR spectra can be assigned to the occurring C–H stretching bands approximately as: (1) first overtone bands of –CH₂ and –CH₃ stretching in the region 5250–6100 cm^{-1} , (2) combinations of vibrational modes 6300–7500 cm^{-1} , and (3) second overtones 8000–8700 cm^{-1} . However, assigning each band and functional group of NIR spectra is difficult compared to other infrared spectra, such as Raman or FTIR.³¹ Hence, the usage of quantitative analyses, such as multivariate calibration of NIR spectra is necessary. A spectral region for building the PLS model was selected (Table 1) and a first derivative preprocessing technique was applied, based on the obtained lowest and best fit given chemometric parameters when compared to baseline correction or the second derivative. Figure 2b shows the optimized spectra for developing the PLS model in the first derivative, where the spectral region between 4000 and 4500 cm^{-1} was eliminated from the calculations to avoid possible interference. In addition, data normalization by mean centering was employed as the first stage in preprocessing to subtract the average from each variable, which ensured that all results would be interpretable in terms of the variation around the mean.

3.2. Calibration and Validation Modeling. Figure 3 shows a graphical representation of each calibration model created using the actual concentration on the x -axis versus the calculated (predicted) concentration on the y -axis, based on the near-infrared (NIR) data. The data employed for the PLS model reference values were based on the exact weight of the improver that was added to the diesel matrix to simultaneously determine the concentrations of all diesel improvers. The PLS models were developed as follows. First, the CLI model was developed using 200 calibration standards with additive contents ranging from 60 to 285 $\text{mg}\cdot\text{kg}^{-1}$, the CFI model was developed using 170 calibration standards (65–215 $\text{mg}\cdot\text{kg}^{-1}$), and the CNI model was developed using 120 calibration standards (75–513 $\text{mg}\cdot\text{kg}^{-1}$). The number of calibration standards used for each model differs owing to the removal of outlying standards and mainly because of the gradual use of additives. For example, initially, only the CLI was added to the diesel specimen, and this was followed by addition of the CFI, and later the CNI. The spectra of the calibration standards containing the same additive concentration were averaged to create the composite standards. Therefore, the PLS models in their final form were composed as follows: the CLI model of 37 calibration standards (Figure 3a), the CFI model of 28 calibration standards (Figure 3b), and the CNI model of 54 calibration standards (Figure 3c), including the composite standards. The corresponding values for the RMSEC parameter, as outlined in Table 1, were found to be 4.2 for the CLI, 4.6 for the CFI, and 5.3 for the CNI. The measure of fit of the calibration model, given by the calculated correlation coefficient (R^2), was >0.99 , depending on the data sample type. This value should be close to 1 to ensure that the maximum variance in the response variable can be attributed to the dataset.

For additional control, cross-validation, i.e., internal validation of the created calibration models, was carried out.

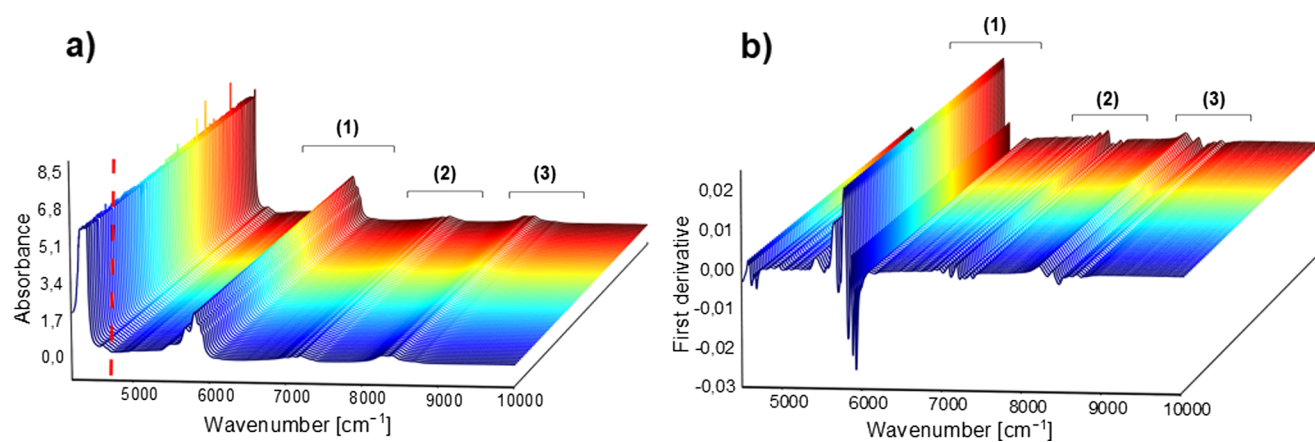


Figure 2. (a) Typical raw absorbance spectra of the samples. (b) First derivative preprocessed NIR spectra used for modeling.

Table 1. Overview of the Chemometric Parameters Employed in the PLS Models

parameter	PLS model		
	CLI	CFI	CNI
spectral region	4501–8600 cm^{-1}	5000–7600 cm^{-1}	4550–9000 cm^{-1}
R^2	0.9978	0.9936	0.9988
RMSEC	4.2	4.6	5.3
RMSECV	21.0	14.5	40.2
LV	9	5	10

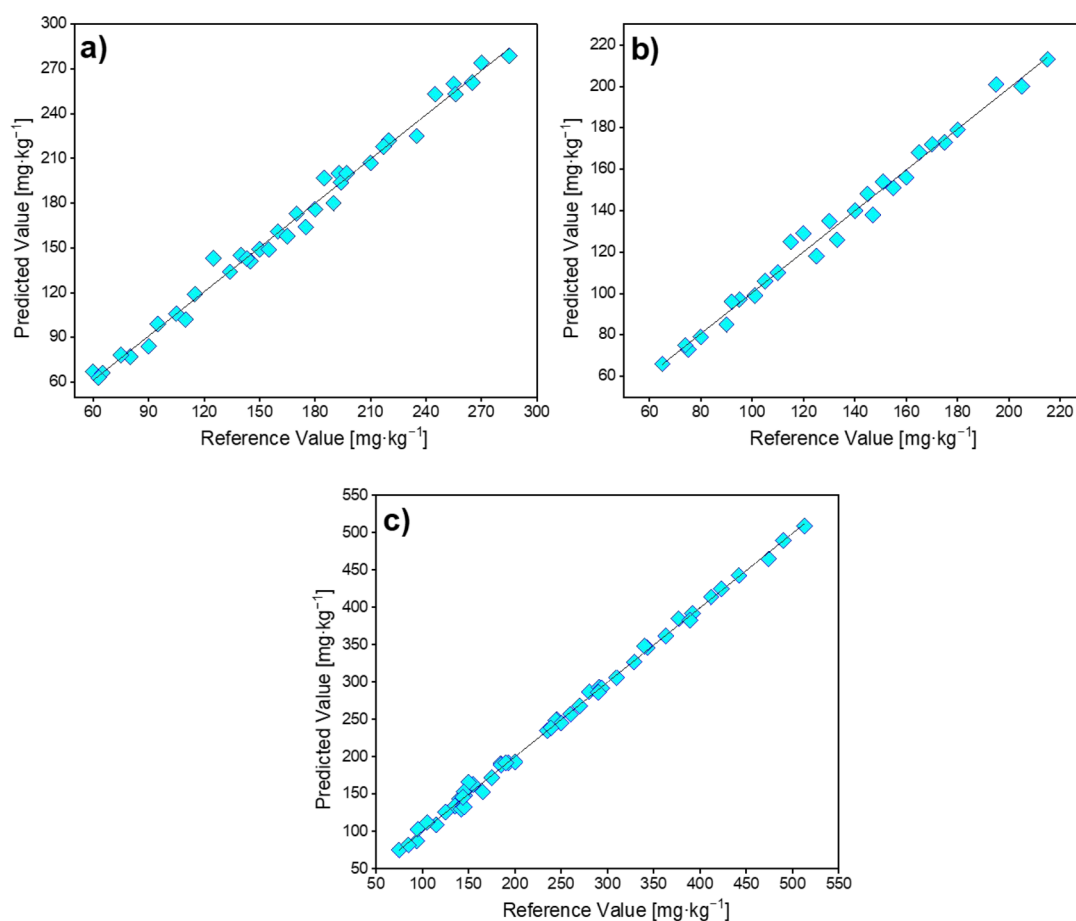


Figure 3. NIR models for PLS regression analysis of each diesel improver containing the composite standards: (a) CLI, (b) CFI, and (c) CNI.

Moreover, the use of this cross-validation approach helps reveal outlying standards. The RMSECV results are shown in

Table 1 for each model. While building the PLS model, the LVs with the lowest RMSECV parameters were preserved until

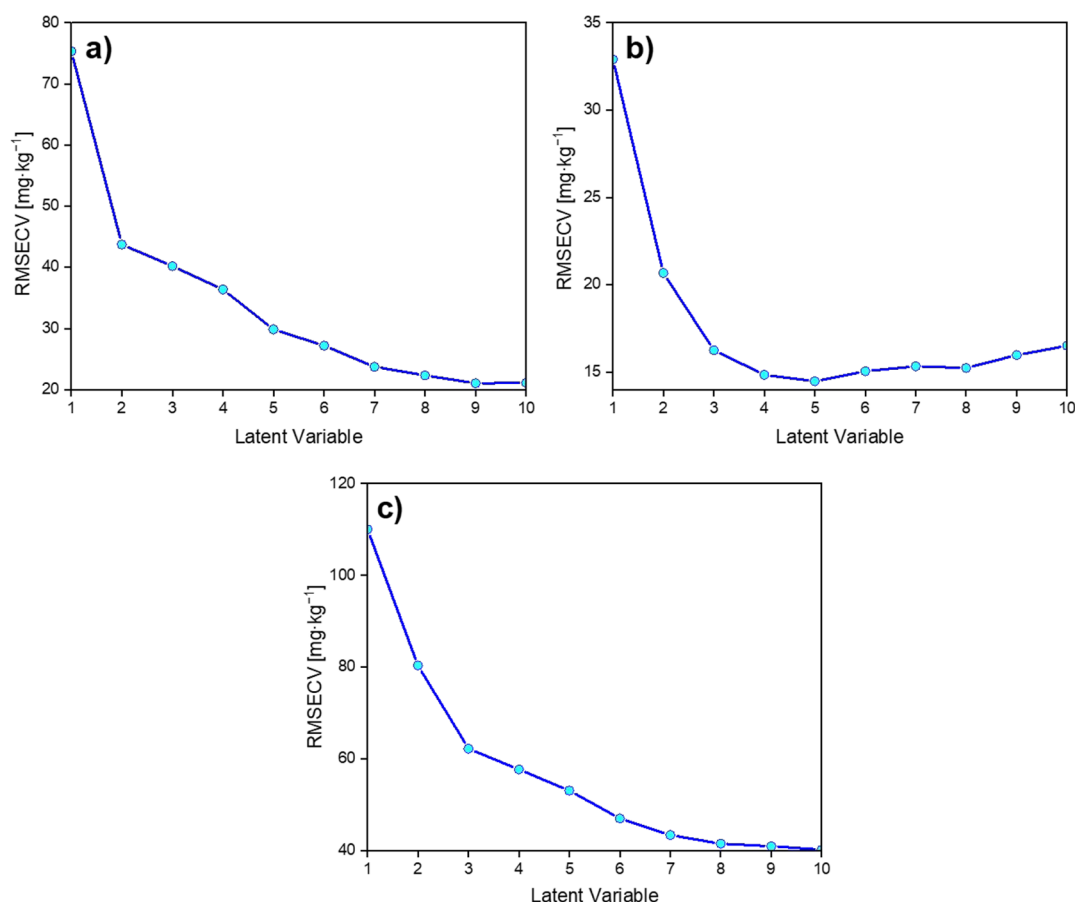


Figure 4. Dependence of the LV on the RMSECV for (a) CLI, (b) CFI, and (c) CNI.

the ratio between the cross-validation and calibration errors (RMSECV/RMSEC) exceeded 10:1. Generally, large differences between the RMSEC and RMSECV indicate a lack of model robustness and the need for greater caution in future predictions. In contrast, a model is considered to be of good quality when the ratio between the RMSEC and RMSECV parameters was not >10:1. In our case, a lower ratio was obtained, which indicates that the number of false-positive results created by the PLS models was minimized. This criterion was empirically established based on previous modeling to avoid overfitting and false-positive results. The dependence of the LVs on the PLS-based RMSECV is presented in Figure 4 and was determined using the minimum PRESS value.³²

The plot showing the dependence of the LV on the RMSECV should take the form of a sharply declining curve, where the optimal factor number is represented by the minimum of the curve. As expected, it was found that upon increasing the factor number, the RMSECV parameter decreased to an essentially constant value. Thus, the optimal LV values for the CLI, CFI, and CNI models were determined to be 9, 5, and 10, respectively. These results highlight the potential of minimal negative influence predictions, as the use of too many factors (i.e., ≥ 20) for PLS modeling can lead to false-positive results.

To further determine the accuracy of the developed PLS models, external validation and repeatability experiments were carried out, as presented in Figure 5 and Table 2, respectively.

Moreover, the external validation data can be found in the Supporting Information. Based on the external validation

dataset, the minimum/maximum absolute differences were determined as follows: CLI minimum = 1 mg·kg⁻¹ for validation standard numbers 9 and 10, CLI maximum = 14 mg·kg⁻¹ for validation standard 4; CFI = zero absolute difference for validation standard number 7, CFI maximum = 14 mg·kg⁻¹ for validation number 2; CNI = zero absolute difference for validation standard number 4, and CNI maximum = 25 mg·kg⁻¹ for validation standard number 6.

Furthermore, the repeatability of the multivariate PLS method (Table 2) was determined based on outlying measurements, using the Dixon's Q-test with a significance level of 0.05 (with a critical value of 0.330 for 15 analyses) and the obtained RSD values. As a result, none of the standards were eliminated. RSD values of 8.1, 7.8, and 7.9% were obtained for the CLI, CFI, and CNI systems, respectively, thereby confirming the reliability of the PLS models. However, it should be noted that a more robust model could yield superior results.

In addition to determining the quality of the PLS models and evaluating whether they are fit for the purpose, the RPD and RER were calculated. Based on previous literature, it is known that an RPD value between 2 and 2.5 indicates that the prediction model is sufficient for determination purposes, while values of 2.5 and ≥ 3 correspond to good and excellent prediction accuracies, respectively.^{33,34} In this study, the RPD values for the PLS models were determined to be 3.1, 2.2, and 2.3 for the CLI, CFI, and CNI systems, respectively, thereby indicating that they are suitable for use in the determination of diesel improvers. However, the prediction performance must be enhanced to achieve higher CFI and CNI values and to

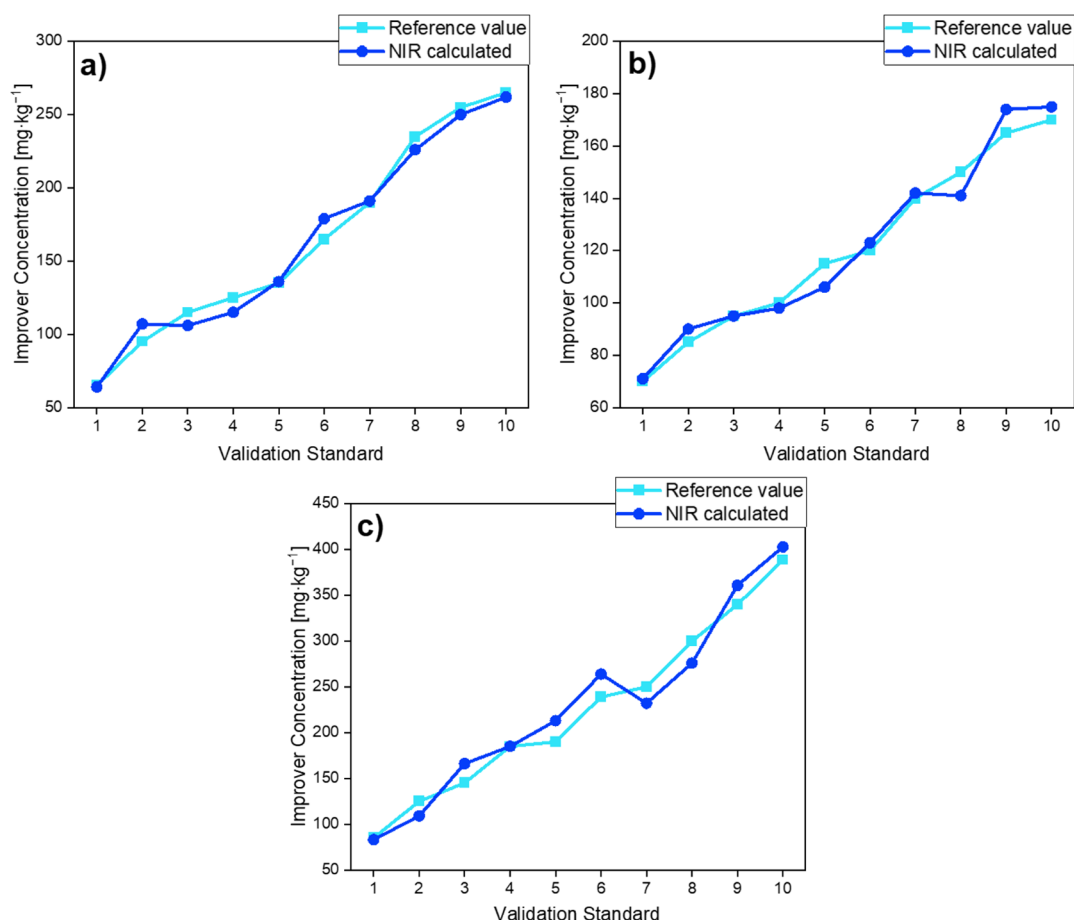


Figure 5. External validation datasets for (a) CLI, (b) CFI, and (c) CNI.

Table 2. Repeatability Test Data for the PLS Models

statistical parameter	value		
	CLI	CFI	CNI
minimum [mg·kg ⁻¹]	118	98	191
maximum [mg·kg ⁻¹]	153	121	242
mean [mg·kg ⁻¹]	137	110	215
reference value [mg·kg ⁻¹]	143	100	190
median [mg·kg ⁻¹]	137	111	216
SD [mg·kg ⁻¹]	11.2	8.5	17.1
RSD (%)	8.1	7.8	7.9
variance [mg·kg ⁻¹]	124	73	292

label these models as excellent for prediction. It should also be noted here that models with RER values >4 are considered suitable for sample screening, while values >10 render the model acceptable for quality control applications, and values >15 allow the model to be employed for quantification purposes; therefore, values >10 are preferred.³⁵ Indeed, the RER values for the CLI, CFI, and CNI systems were calculated to be 10.7, 10.3, and 12.8, respectively, thereby further confirming the suitability of the developed models.

Here, we performed cost analysis of the mentioned additives according to the information of individual suppliers. CLI and CFI groups of additives are currently (2022) commercially available at a price level of around 3400–3900 EUR per ton. In the case of CNI, it is an amount of 1900–2100 EUR/ton. It should be mentioned that the last year marked a significant price increase, especially in the case of CLI additives, for which

the price was increased by 119%. The smallest price increase was for additives of the CNI group (+18%), probably due to the fact that it is a pure chemical (2-EHN).

Taking into account the current price level and the RSD (8%), it would be possible to calculate potential savings in the accuracy of dosing of individual additives. For these calculations, the verified maximum of the tested ranges was considered, which at 8% is 23 mg/kg for CLI; 17 mg/kg for CFI, and 41 mg·kg⁻¹ for CNI. Potential savings when using the mentioned PLS model then reach up to 242 EUR per ton of diesel fuel produced.

Previously, Velvarká et al.³⁶ predicted the concentration of one additive in diesel fuel, namely, CFIs, using NIR spectroscopy with the PLS model developed in the range of 15–325 mg·kg⁻¹ and with the following parameters calculated by their PLS model; RMSEC (11.9 mg·kg⁻¹), RMSECV (28.4 mg·kg⁻¹), and R² (0.9880). Moreover, they reported RPD 2.7, RER 10.9, and the maximum absolute difference between the actual value and the NIR value for CFI 17 mg·kg⁻¹. Areas where significant differences have been found in comparison to our PLS model include RMSEC (5.3 mg·kg⁻¹), RMSECV (14.5 mg·kg⁻¹), and R² (0.9936), whereas the PLS model in this study performed well over a lower concentration range 65–215 mg·kg⁻¹. Furthermore, we demonstrate a CFI maximum absolute difference of 14 mg·kg⁻¹. Based on these results, it is apparent that our PLS model was superior to that of Velvarká et al. However, it should be noted that these authors reported better RPD and RER performance efficiencies of 2.7 and 10.9, respectively, which are superior to our values

of 2.2 and 10.3; these differences may have been due to the lower range of additive concentrations used in this study. However, as we mentioned before, they predicted concentration just for one diesel improver in a larger range, in contrast, we determined three additives at the same time in one diesel fuel sample, which is more suitable for saving time and costs.

In addition, Vrtiška and Šimáček³⁷ employed FTIR and PLS models to predict the content of CNI 2-ethylhexyl nitrate (EHN) in the range of 0–2436 mg·kg⁻¹ in diesel/biodiesel blends with a mean error of 32 mg·kg⁻¹. By contrast, we predict the CNI in the smaller range of 75–513 mg·kg⁻¹.

Nevertheless, despite some of the beneficial properties of the previously described PLS models by authors, our model stands out due to the fact that we determined the contents of three types of diesel improvers in the diesel matrix, thereby rendering our model more desirable for online monitoring purposes. It should also be noted that the investigation of a higher concentration range could potentially yield more desirable results, and this will be investigated in the future by our group.

4. CONCLUSIONS

NIR spectroscopy was used to determine the concentrations of the three types commonly used diesel improvers, including a CLI, a CFI, and a CNI. The developed PLS models were evaluated using a range of chemometric parameters, correlation coefficients, the RMSEC, RMSECV, and LVs. To determine the quality of the developed PLS models, external validation and repeatability experiments were performed, wherein an acceptable RSD of 8% was obtained. Moreover, we acquired an RPD >2 and an RER >10 for each PLS model. Although a more robust model would be expected to yield superior results, the current PLS models are highly accurate for online monitoring purposes.

Our results highlight the potential of NIR spectroscopy to be used as a fast, inexpensive, and efficient tool for the determination of concentrations of three diesel improvers in diesel fuel at the same time. In addition, we recommend NIR spectroscopy as a suitable technique for application in refinery production; specifically, it would be possible to monitor the content of additives in diesel fuel online either during or after blending. In addition, this monitoring only requires a NIR spectrometer instead of several devices and techniques, which brings advantages in terms of rapid response to avoid fuel overdoses, thus saving costs. As further variants following this study, it would be possible to verify whether it is possible to determine a larger number of additives at the same time or whether three types of improvers can also be analyzed with a different matrix or a different ratio of diesel to biomaterial.

■ ASSOCIATED CONTENT

SI Supporting Information

The Supporting Information is available free of charge at <https://pubs.acs.org/doi/10.1021/acsomega.2c06845>.

Data used for NIR models development and for external validation of each diesel improver (PDF)

■ AUTHOR INFORMATION

Corresponding Author

Ivana Hradecká – ORLEN UniCRE a.s., 400 01 Ústí nad Labem, Czech Republic; Department of Chemistry, Faculty of

Agrobiology, Food and Natural Resources, Czech University of Life Sciences Prague, 165 00 Prague, Czech Republic;
orcid.org/0000-0002-3860-2029;
Email: ivana.hradecka@orlenuicre.cz

Authors

Aleš Vráblík – ORLEN UniCRE a.s., 400 01 Ústí nad Labem, Czech Republic

Jakub Frątczak – ORLEN UniCRE a.s., 400 01 Ústí nad Labem, Czech Republic; Department of Chemistry, Faculty of Agrobiology, Food and Natural Resources, Czech University of Life Sciences Prague, 165 00 Prague, Czech Republic

Nikita Sharkov – ORLEN UniCRE a.s., 400 01 Ústí nad Labem, Czech Republic

Radek Černý – ORLEN UniCRE a.s., 400 01 Ústí nad Labem, Czech Republic

Vladimír Hömig – Department of Chemistry, Faculty of Agrobiology, Food and Natural Resources, Czech University of Life Sciences Prague, 165 00 Prague, Czech Republic

Complete contact information is available at:

<https://pubs.acs.org/10.1021/acsomega.2c06845>

Author Contributions

All authors have given approval to the final version of the manuscript.

Notes

The authors declare no competing financial interest.

■ ACKNOWLEDGMENTS

The work is a result of the project which was carried out within the financial support of the Ministry of Industry and Trade of the Czech Republic with institutional support for long-term conceptual development of research organization. The result was achieved using the infrastructure included in the project Efficient Use of Energy Resources Using Catalytic Processes (LM2018119) which has been financially supported by MEYS within the targeted support of large infrastructures.

■ ABBREVIATIONS

ASTM	American Society for Testing Materials
CFI	cold-flow improver
CFPP	cold filter plugging point
CLI	conductivity–lubricity improver
CNI	cetane number improver
EHN	2-ethylhexyl nitrate
EN	European standard
HFRR	high-frequency reciprocating rig
LV	latent variable
NIR	near-infrared
PLS	partial least squares
PRESS	predicted residual error sum of squares
RER	ratio of error range
RMSEC	root mean square error of calibration
RMSECV	root mean square error of cross-validation
RPD	ratio of prediction to deviation
RSD	residual standard deviation
WAFI	wax antisetling flow improvers

■ REFERENCES

(1) Fayyazbakhsh, A.; Pirouzfard, V. Comprehensive overview on diesel additives to reduce emissions, enhance fuel properties and improve engine performance. *Renew. Sustainable Energy Rev.* **2017**, *74*, 891–901.

- (2) Naga Venkata Siddartha, G.; Siva Ramakrishna, C.; Kumar Kujur, P.; Anupam Rao, Y.; Dalela, N.; Singh Yadav, A.; Sharma, A. Effect of fuel additives on internal combustion engine performance and emissions. *Mater. Today: Proc.* **2022**, *63*, A9–A14.
- (3) Nagappan, M.; Devaraj, A.; Babu, J. M.; Vibhav Saxena, N.; Prakash, O.; Kumar, P.; Sharma, A. Impact of additives on Combustion, performance and exhaust emission of biodiesel fueled direct injection diesel engine. *Mater. Today: Proc.* **2022**, *62*, 2326.
- (4) Toscano, G.; Leoni, E.; Gasperini, T.; Picchi, G. Performance of a portable NIR spectrometer for the determination of moisture content of industrial wood chips fuel. *Fuel* **2022**, *320*, No. 123948.
- (5) Santos, F. D.; Santos, L. P.; Cunha, P. H. P.; Borghi, F. T.; Romão, W.; de Castro, E. V. R.; de Oliveira, E. C.; Filgueiras, P. R. Discrimination of oils and fuels using a portable NIR spectrometer. *Fuel* **2021**, *283*, No. 118854.
- (6) Liu, S.; Wang, S.; Hu, C.; Zhan, S.; Kong, D.; Wang, J. Rapid and accurate determination of diesel multiple properties through NIR data analysis assisted by machine learning. *Spectrochim. Acta, Part A* **2022**, *277*, No. 121261.
- (7) Bukkarapu, K. R.; Krishnasamy, A. Predicting engine fuel properties of biodiesel and biodiesel-diesel blends using spectroscopy based approach. *Fuel Process. Technol.* **2022**, *230*, No. 107227.
- (8) Hradecká, I.; Velvarská, R.; Janková, K. D.; Vráblik, A. Rapid determination of diesel fuel properties by near-infrared spectroscopy. *Infrared Phys. Technol.* **2021**, *119*, No. 103933.
- (9) Buendia Garcia, J.; Lacoue-Negre, M.; Gornay, J.; Mas Garcia, S.; Bendoula, R.; Roger, J. M. Diesel cetane number estimation from NIR spectra of hydrocracking total effluent. *Fuel* **2022**, *324*, No. 124647.
- (10) Liu, S.; Wang, S.; Hu, C.; Qin, X.; Wang, J.; Kong, D. Development of a new NIR-machine learning approach for simultaneous detection of diesel various properties. *Measurement* **2022**, *187*, No. 110293.
- (11) Palou, A.; Miró, A.; Blanco, M.; Larraz, R.; Gómez, J. F.; Martínez, T.; González, J. M.; Alcalá, M. Calibration sets selection strategy for the construction of robust PLS models for prediction of biodiesel/diesel blends physico-chemical properties using NIR spectroscopy. *Spectrochim. Acta, Part A* **2017**, *180*, 119–126.
- (12) Tasić, I.; Tomić, M. D.; Aleksić, A. L.; Đurišić-Mladenović, N.; Martinović, F. L.; Micić, R. D. Improvement of low-temperature characteristics of biodiesel by additivation. *Hem. Ind.* **2019**, *73*, 103–114.
- (13) Yang, T.; Wu, J.; Yuan, M.; Li, X.; Yin, S.; Su, B.; Yan, J.; Lin, H.-L.; Xue, Y.; Han, S. Influence of polar groups on the depressive effects of polymethacrylate polymers as cold flow improvers for diesel fuel. *Fuel* **2021**, *290*, No. 120035.
- (14) Brown, G. I.; Tack, R. D.; Chandler, J. E. *An Additive Solution to the Problem of Wax Settling in Diesel Fuels* (No. CONF-8810120-) ; Society of Automotive Engineers: Warrendale, PA, 1988.
- (15) Prathima, A.; Karthikeyan, S.; Radhi Devi, K.; Usha, K.; Shanthi, M. Environmental effect of lubricity additives through dielectric molecular parameters. *Mater. Today Proc.* **2020**, *33*, 3658–3663.
- (16) Kuszewski, H.; Jaworski, A.; Ustrzycki, A. Lubricity of ethanol–diesel blends – Study with the HFRR method. *Fuel* **2017**, *208*, 491–498.
- (17) EN 590:2013+A1:2017 . *Automotive Fuels - Diesel - Requirements and Test Methods*.
- (18) ASTM D6079-18 . *Standard Test Method for Evaluating Lubricity of Diesel Fuels by the High-Frequency Reciprocating Rig (HFRR)*; West Conshohocken, PA, 2018.
- (19) Hsieh, P. Y.; Bruno, T. J. A perspective on the origin of lubricity in petroleum distillate motor fuels. *Fuel Process. Technol.* **2015**, *129*, 52–60.
- (20) Sánchez-Delgado, R. A.1.27 - Hydrodesulfurization and Hydrodenitrogenation. In *Comprehensive Organometallic Chemistry III*, Mingos, D. M. P., Crabtree, R. H. Eds.; Elsevier, 2007; pp. 759–800.
- (21) ASTM D613-01. *Standard Test Method For Cetane Number Of Diesel Fuel Oil*; West Conshohocken, PA, 2001
- (22) Atmanli, A. Effects of a cetane improver on fuel properties and engine characteristics of a diesel engine fueled with the blends of diesel, hazelnut oil and higher carbon alcohol. *Fuel* **2016**, *172*, 209–217.
- (23) Canoira, L.; Alcántara, R.; Torcal, S.; Tsiouvaras, N.; Lois, E.; Korres, D. M. Nitration of biodiesel of waste oil: Nitrated biodiesel as a cetane number enhancer. *Fuel* **2007**, *86*, 965–971.
- (24) Hanlon, J. V.; Hinkamp, J. B. Desensitized cetane improvers. United States US4473378A, 1984.
- (25) Seemuth, P. D. Cetane improver composition. United States US4536190A, 1985.
- (26) Li, R.; Wang, Z.; Ni, P.; Zhao, Y.; Li, M.; Li, L. Effects of cetane number improvers on the performance of diesel engine fuelled with methanol/biodiesel blend. *Fuel* **2014**, *128*, 180–187.
- (27) ASTM D4057-22 . *Standard Practice for Manual Sampling of Petroleum and Petroleum Products*; West Conshohocken, PA, 2022.
- (28) de Faria, B. D. F. H.; Santana Barbosa, P.; Valente Roque, J.; de Cássia Oliveira Carneiro, A.; Rousset, P.; Candelier, K.; Francisco Teófilo, R. Evaluation of weight loss and high heating value from biomasses during fungal degradation by NIR spectroscopy. *Fuel* **2022**, *320*, No. 123841.
- (29) Fearn, T. Assessing calibrations: sep, rpd, rer and r 2. *NIR News* **2002**, *13*, 12–13.
- (30) Williams, P. C.; Sobering, D.; Davies, A.; Williams, P. Near infrared spectroscopy: the future waves. In *Proceedings of the 7th International Conference on Near Infrared Spectroscopy*, 1996; p. 742.
- (31) Salzer, R. Practical Guide to Interpretive Near-Infrared Spectroscopy. By Jerry Workman, Jr. and Lois Weyer. *Angew. Chem. Int. Ed.* **2008**, *47*, 4628–4629.
- (32) Wong, T.-T. Performance evaluation of classification algorithms by k-fold and leave-one-out cross validation. *Pattern Recognit.* **2015**, *48*, 2839–2846.
- (33) Nicolai, B. M.; Beullens, K.; Bobelyn, E.; Peirs, A.; Saeys, W.; Theron, K. I.; Lammertyn, J. Nondestructive measurement of fruit and vegetable quality by means of NIR spectroscopy: A review. *Postharvest Biol. Technol.* **2007**, *46*, 99–118.
- (34) Williams, P. C.; Sobering, D. How do we do it: a brief summary of the methods we use in developing near infrared calibrations. In *Near infrared spectroscopy: The future waves*; NIR Publications: Chichester, 1996; pp. 185–188.
- (35) Hayes, D. M.; Hayes, M.; Leahy, J. Use of near infrared spectroscopy for the rapid low-cost analysis of waste papers and cardboards. *Faraday Discuss.* **2017**, *202*, 465–482.
- (36) Velvarská, R.; Vráblik, A.; Hidalgo-Herrador, J. M.; Černý, R. Near-infrared spectroscopy to determine cold-flow improver concentrations in diesel fuel. *Infrared Phys. Technol.* **2020**, *110*, No. 103445.
- (37) Vrtiška, D.; Šimáček, P. Prediction of 2-EHN content in diesel/biodiesel blends using FTIR and chemometrics. *Talanta* **2018**, *178*, 987–991.